Kinetic electron emission from clean polycrystalline gold induced by impact of slow C^+, N^+, O^+, Ne^+, Xe^+, and Au^+ ions

Jan Lörinčík,[1] Zdeněk Šroubek,[2] Hannes Eder,[3] Friedrich Aumayr,[3] and Hannspeter Winter[3]
[1]*J. Heyrovsky Institute of Physical Chemistry, Academy of Sciences of the Czech Republic, Dolejskova 3, 18223 Praha, Czech Republic*
[2]*Institute of Radio Engineering and Electronics, Academy of Sciences of the Czech Republic, Chaberska 57, 18251 Praha, Czech Republic*
[3]*Institut für Allgemeine Physik, TU Wien, Wiedner Hauptstrasse 8-10, A-1040 Wien, Austria*
(Received 8 February 2000; revised manuscript received 17 April 2000)

Ion-induced kinetic electron emission is commonly attributed to collisions of an energetic projectile with quasifree electrons, and to the promotion of atomic levels in binary collisions of the projectile with atomic particles in the solid. The contribution of the promotion processes to the electron emission has been estimated theoretically for all studied systems from molecular-orbital correlation diagrams. As quasifree electron collisional excitations have a sharp threshold at relatively high velocities of the projectiles, their contribution to the electron emission at lower impact velocities should be negligible. We will show, however, that the partial localization of the quasifree electrons due to the presence of the solid surface ''washes out'' this sharp threshold. This can lead to one-electron excitations at low impact velocities that may be more significant than excitations due to promotion. At the lowest impact velocities the electron emission yields conspicuously level off in some studied cases. Such behavior cannot be reconciled with any existing one-electron model (including the one proposed here), as they all predict a rapid decrease of the electron emission with decreasing impact velocity. In this paper we interpret the leveling-off of the yield in terms of a many-electron excitation mechanism, based on the assumption of spatial and temporal localizations of electronic excitation in the impact zone. The models discussed in this paper will be compared with experimental data on kinetic electron emission from polycrystalline gold bombarded by C^+, N^+, O^+, Ne^+, Ne^0, Xe^+, and Au^+, with kinetic energies below ~15 keV, and perpendicular incidence on the surface.

I. INTRODUCTION

When an atomic particle impinges upon a solid surface, electrons of the solid or of the particle may be excited and emitted into the vacuum. This phenomenon is called particle-induced electron emission (PIE)[1–3] or ion-induced electron emission, because most of the relevant experiments were done with ions as primary particles. If the projectile carries sufficient potential energy, i.e., if it is a singly charged ion with higher ionization potential or a multiply charged ion, Auger neutralization of such projectiles near the surface leads to the so-called potential electron emission (PE). This process does not require any kinetic projectile energy, and is often dominant for PIE at very low impact velocity. Another contribution to PIE is the so-called kinetic electron emission (KE), where the most important physical influence is due to the kinetic energy of the impinging particle. KE is subject to an impact velocity threshold below which no contribution to PIE can occur. Often both PE and KE processes arise due to the impact of a projectile, and it depends on the particular projectile-target combination and the impact velocity which of the two mechanisms is the more important.[1–3]

In KE ejected electrons are generated at or below the surface in collisions of the projectile with target atoms, or directly with the valence electrons of the solid;[1–3] the most critical parameter is the projectile velocity. There are two established mechanisms of KE. In the first one the valence electrons of the solid become excited in binary collisions with the projectile moving in an idealized Fermi electron gas, and are thereby ejected into the vacuum.[4] This process, which we will call ''electronic KE (eKE)'' in this paper, is subject to a threshold impact velocity $v_{\mathrm{th},e}$ below which no electron emission should be possible;[5]

$$v_{\mathrm{th},e}=\frac{1}{2}v_F\left[\left(1+\frac{W}{E_F}\right)^{1/2}-1\right], \tag{1}$$

where W, E_F, and v_F are the work function, the Fermi energy, and the Fermi velocity of the target, respectively. For example, the threshold velocity for impact of Au^+ on a clean Au surface would correspond to 60-keV kinetic energy. It is therefore surprising to find considerable KE for 3-keV Au^+ impinging on Au.[6] KE below the impact threshold velocity $v_{\mathrm{th},e}$ was observed previously for many other collision systems. It has been called ''subthreshold KE,'' and becomes gradually more important for heavier projectiles.[3,7,8]

Until recently, the only available explanation for the subthreshold KE was given in terms of the promotion model for KE which involves close binary collisions between projectiles and target atoms (or mutual target atom collisions) at or below the surface. These collisions temporarily create (quasi-)molecules in which some electronic levels may be sufficiently strongly promoted to higher orbital energies, and thus give rise to electron emission in subsequent deexcitation steps.[9,10] This KE mechanism will be called ''promotional KE (pKE)'' in our paper. The pKE process is characterized by a threshold impact velocity $v_{\mathrm{th},p}$ or kinetic energy $E_{\mathrm{th},p}$ which strongly depends on the particular com-

bination of the collision partners. The threshold energy $E_{th,p}$ can be experimentally determined, and can be theoretically estimated from the analysis of molecular-orbital (MO) correlation diagrams. However, nonvanishing KE yields have been often observed not only below $v_{th,e}$ but also well below $v_{th,p}$ and, thus, in such cases, the subthreshold KE cannot be due to the pKE mechanism.[7,11,12]

It is obvious that the sharp threshold of eKE, defined by $v_{th,e}$, is due to the idealized concept of plane-wave-like free electrons and of a particle moving with a constant velocity, which needs to be re-examined. When the electrons are partially localized or the particle does not move along a straight trajectory with a constant speed, a smearing out of the threshold takes place, and electrons can be emitted at energies below an energy corresponding to $v_{th,e}$. The localization of valence-band electrons can be due to:

(a) the *d*-like character of the valence band,[13]

(b) the spatial confinement of valence electrons by the presence of the solid surface,[12]

(c) the admixture of inner-shell wave functions to the valence electron wave function by the orthogonalization procedure.

The localized character of valence *d* electrons was already used in Ref. 13 to identify the mechanism for KE from grazing collisions of keV protons with a single-crystal Cu surface. The electrons are assumed to be excited directly from the Cu *d* band by several distant collisions of the neutralized hydrogen projectile. Recently an attempt was made to interpret the subthreshold KE from Au bombarded by Ne^+ and Ne^0 (Ref. 12) using a mechanism in which valence electrons are partially localized (semilocalized) due to their confinement by the surface of the solid. This kind of collision involves a nonclassical process with no cutoff velocity but rather a smooth exponential decay toward a low impact velocity. In this paper we label this KE mechanism as ''surface-assisted KE (sKE).'' As will be shown in Sec. IV a good fit of the sKE model predictions to the measured KE yields for the bombardment of clean Au by light projectiles $Ne^{+,0}$, N^+, O^+, and C^+ could be obtained in the impact energy range from a few hundred eV up to 15 keV. However, for the collision systems Xe^+-Au, and Au^+-Au,[6] the yield shows a gradually slower decay for lower velocities. This behavior cannot be explained by any of the three mechanisms for KE mentioned so far, i.e., eKE, pKE, and sKE. In this paper we present a many-electron mechanism for KE in the very low impact velocity regime for explaining these recent measurements. In the next paragraph we will utilize MO correlation diagrams for C-Au, N-Au, O-Au, Ne-Au, Xe-Au, and Au-Au collisions in order to perform a semiquantitative analysis for the probability of pKE for these collision systems.

II. ANALYSIS OF MO CORRELATION DIAGRAMS FOR C-Au, N-Au, O-Au, Ne-Au, Xe-Au, and Au-Au

The main reason for the analysis of the respective MO correlation diagrams in this work is to show that the pKE model cannot yield sufficient explanation of the KE yield at low impact energies, and that there is a need for new KE mechanisms. The MO correlation diagrams for the neutral systems of Ne-Au, O-Au, N-Au, C-Au, Xe-Au, and Au-Au are shown in Figs. 1(a)–1(f). Atomic units for distance (1 a.u.$\sim$0.053 nm), energy (1 a.u.$\sim$27.2 eV) and velocity (1 a.u.$\sim 2.18\times 10^6$ m/s) are used throughout this paper. The diagrams in Fig. 1 were calculated using the Hartree-Fock method and the computer code GAUSSIAN 98.[14] As a basis set, LANL2DZ (Ref. 15) was used for all systems.

The results of the analysis of the MO correlation diagrams in Figs. 1(a)–1(f) are summarized in Table I. The identified promoted diabatic levels (applying Barat-Lichten correlation rules) and the corresponding atomic levels in the separated-atom (SA) limit are listed in columns 2 and 3. Due to the small energy splitting at the avoided crossings of the 14σ and 15σ levels at internuclear distances of $\sim$1.6 a.u., the atomic levels in the SA limit in Figs. 1(b)–1(d) were identified as $2s$ rather than $2p$. The promoted levels merge into the continuum above the vacuum level at internuclear distances r_0 (column 4). Using the Moliere interatomic potential, we estimated the minimal kinetic energy E_0 (column 5) required for reaching these internuclear distances. But if we take this energy as an estimate for $E_{th,p}$, then we must bear in mind that such values for $E_{th,p}$ may be strongly underestimated for two main reasons: (i) r_0 is the turning point corresponding to the initial energy E_0, and therefore the velocity at this point is zero; and (ii) E_0 was estimated only for head-on collisions.

In Ref. 12 an attempt was made to evaluate how much these E_0 values are underestimated. A semiquantitative analysis of the relevant avoided crossings was performed, and the value for $E_{th,p}$ was calculated for the Ne-Au system. That $E_{th,p}$ value was larger by $\sim$60% than the E_0 value, and it depends on the preset criterion for the diabatic character of the relevant avoided crossing. For the purpose of this work the $E_{th,p}$ values derived from E_0 are sufficient, and there is no need for an additional analysis. In some cases the present $E_{th,p}$ estimate can be confronted with experiments. In Ref. 16 electron energy spectra for Xe^+ impact on gold were measured for several projectile energies between 0.5 and 8 keV. Up to 2 keV these spectra remain structureless, but from 3 keV up to 8 keV a bump appeared at an electron energy of $\sim$7 eV, for which no explanation was provided. It seems from our estimate that some (so far unknown) process may start up at $E_{th,p}\approx 2.5$ keV. The promotion of the $7g\sigma$(Au $5d$) level can create a vacancy in the Au $5d$ level, which may be transferred by vacancy sharing into the Xe $5p$ level. De-excitation of the latter could give rise to the above-mentioned spectral feature in the ejected-electron energy distributions. For Au-Au we obtained only an order of magnitude estimate for the value of $E_{th,p}$.

When speaking about threshold values, it is important to realize that the pKE model in principle does not predict any sharp threshold as in the case of eKE [see Eq. (1)]. The pKE involves a nonadiabatic process with an extremely steep dependence on the impact velocity; it may have a general functional dependence of, e.g., $\exp(-\text{const}/v)$ with a large value for the constant in the exponent.

All MO correlation diagrams were calculated for free diatomic systems. The influence of the solid on the discussed promotion processes depends on the degree of delocalization of molecular levels which form the valence band of the solid. Qualitatively a totally delocalized level means no promotion,

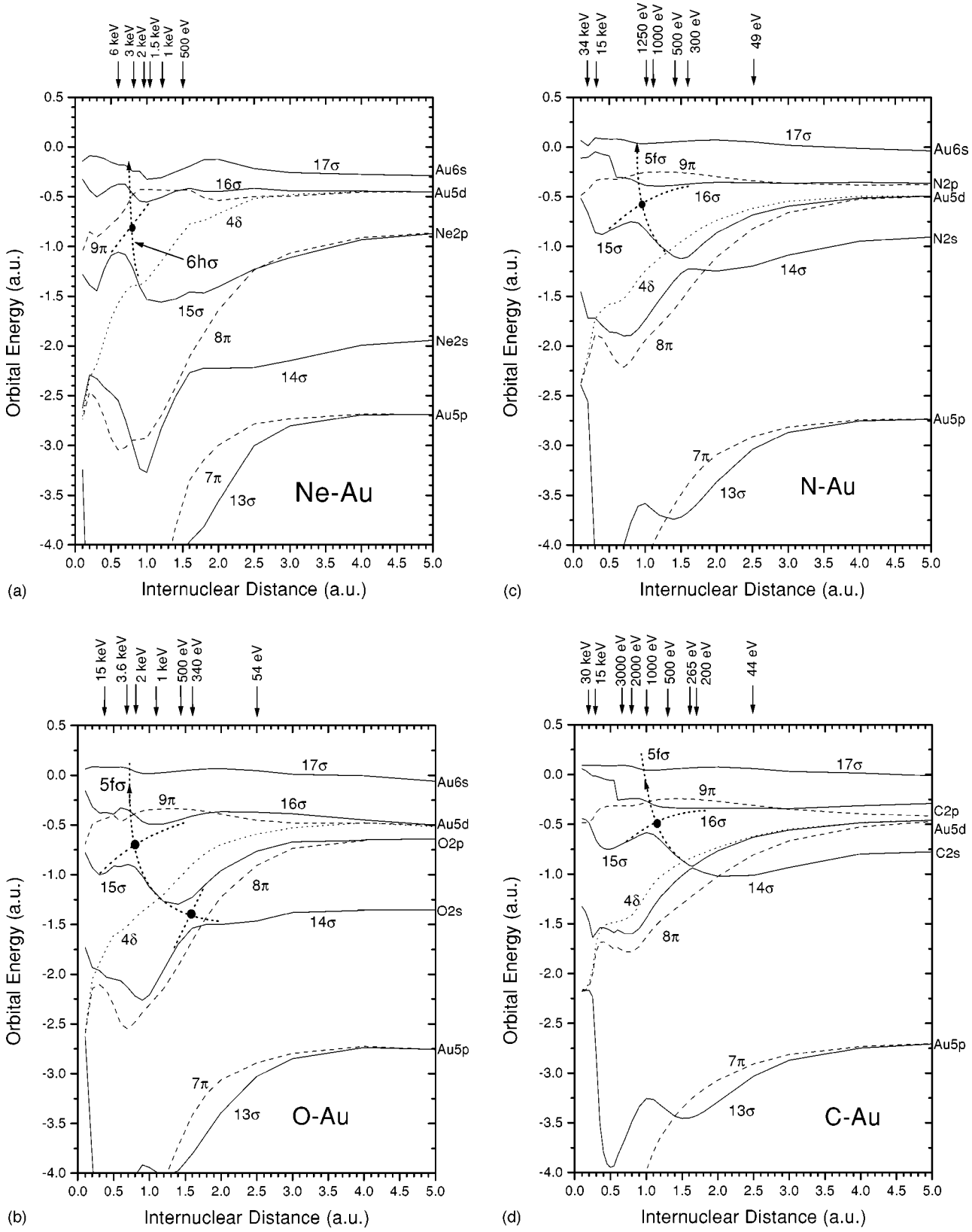

FIG. 1. Adiabatic molecular-orbital (MO) correlation diagrams for the selected orbitals of (a) Ne-Au (Ref. 12) (b) O-Au, (c) N-Au, (d) C-Au, (e) Xe-Au, and (f) Au-Au as calculated by the Hartree-Fock method. Solid lines are σ-levels, dashed lines π levels and dotted lines δ levels; the levels for the separated-atom limit are indicated on the right-hand side of the diagram. The dotted heavy curve with an arrow shows the promotion of diabatic levels into continuum. The adiabatic levels are labeled in the MO notation: The lowest orbital of a given symmetry is numbered 1, and numbering continues in ascending order up to higher energies. For Au-Au an additional notation is used to indicate the symmetry of the wave functions [g for symmetric (''gerade'') and u for asymmetric (''ungerade'') wave functions]. Bars on top of the diagram indicate projectile energies corresponding to the distances of closest approach which can be read on the x axis.

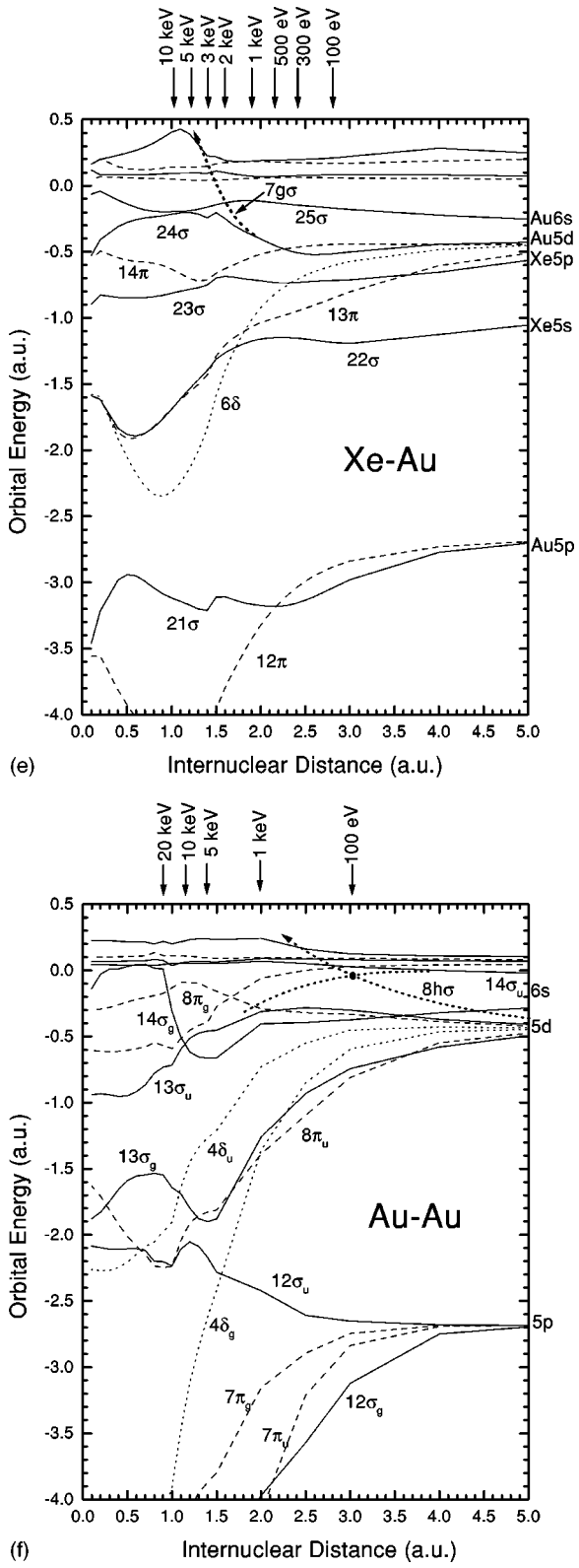

FIG. 1. (*Continued*).

and a localized level means efficient promotion if there is enough collisional energy available. This is a consequence of the Pauli exclusion principle. Following this reasoning the 17σ levels in Figs. 1(a)–1(d), and the 25σ, and $14\sigma_u$, and $14\sigma_g$ levels in Figs. 1(e) and 1(f) were disregarded in the semiquantitative analysis, because their SA limit is a fully delocalized Au $6s$ level. The Au $5d$ level of the valence band is an intermediate case, and can be considered as semilocalized (because of the relatively narrow d-band part of the valence band).

TABLE I. Summary of the analysis of MO correlation diagrams.

System	Promoted diabatic level[a]	SA-limit level	r_0[b] in a.u.	E_0[c] in keV	$E_{\mathrm{th},p}$[d] in keV	$E_{\mathrm{th},e}$ in keV
Ne-Au	$6h\sigma$	Ne$2p$	0.80	3.0	>3.0	6.0
O-Au	$5f\sigma$	O$2s$	0.75	2.8	>2.8	4.8
N-Au	$5f\sigma$	N$2s$	0.90	1.6	>1.6	4.2
C-Au	$5f\sigma$	C$2s$	0.95	1.2	>1.2	3.6
Xe-Au	$7g\sigma$	Au$5d$	1.50	2.5	>2.5	40.0
Au-Au	$8h\sigma$	Au$5d$	3.00	0.1	~ 10[e]	60.0

[a]According to Barat-Lichten correlation rules.
[b]The distance of merging of the promoted diabatic level to the continuum.
[c]The estimate of the kinetic energy required to just reach r_0, i.e., the velocity at r_0 would be zero for this energy.
[d]The values for $E_{\mathrm{th},p}$ are underestimated (cf. the text), which is indicated by ''$>$.''
[e]An order of magnitude estimate not related to the value of E_0.

As a main result of our semiquantitative analysis of the MO correlation diagrams, we obtained estimates for the threshold energies of the pKE process (column 6 in Table I). For comparison, the values for $E_{\mathrm{th},e}$ obtained from Eq. (1) are listed in the last column of Table I. Although our estimated $E_{\mathrm{th},p}$ values are lower than the respective $E_{\mathrm{th},e}$ values, there are reliable experiments on the above studied systems[6,7,16] where a substantial subthreshold KE has been observed at still lower energies than $E_{\mathrm{th},p}$. Apparently, neither the pKE model nor the eKE model can provide a satisfactory interpretation of these experimental data. We will show in Sec. IV that our recently suggested sKE mechanism can provide a reasonable explanation for this subthreshold KE for the studied collision systems. However, before we start to discuss the application of the sKE mechanism, we will briefly describe this model.

III. SURFACE-ASSISTED KE

For systems where the difference between the ionization energy of the projectile and the Fermi energy is small, the sKE process can be modeled by the dynamic Anderson-Newns Hamiltonian. Using this formalism, characteristic features of PIE from Al bombarded by Li^+ were recently described.[17] The advantage of such an approach is that the empirical parameters used for a description of the electron emission can be deduced from other ion-surface experiments.[17] In the Anderson-Newns Hamiltonian the direct interaction $V_{kk'}$ produced by the particle between the occupied $|k'\rangle$ and the unoccupied $|k\rangle$ levels of the continuum is neglected, because it is not directly related to the charge states of scattered particles where this description is mostly applied. This interaction may, however, also be responsible for the eKE processes, and in many cases should be included. In our case the ionization potentials of the projectiles are high, we neglect any transfer of electrons from the projectiles to the substrate (a characteristic of the Anderson-Newns Hamil-

tonian), and we assume that only $V_{kk'}$ are relevant. The time-varying surface interaction is modeled in our approach by the matrix elements $V_{kk'}=\langle k|V(r)|k'\rangle$, where k and k' are the free-electron-like wave functions of the solid and $V(r)$ is the perturbing potential caused by the particle. Inside the solid these matrix elements are responsible for the electronic stopping at low energies, and depend on time as $\langle k|V(\mathbf{r}-\mathbf{v}t)|k'\rangle$, where $\mathbf{v}$ is the velocity of the projectile. If the potential is an s scatterer, the matrix elements $V_{kk'}$ are assumed to be independent of k and k', i.e., $V_{kk'}=V$, and the relation for the stopping power is given by[18]

$$\frac{dE}{dx}=\frac{\pi}{3}\rho^2V^2k_F^2v, \tag{2}$$

where ρ is the electronic density of states at the Fermi energy. At the surface of the solid the potential V should change smoothly from its full value inside the solid to zero outside the solid. The spatial dependence of V transforms to the time dependence as the particle moves toward or away from the surface. When the potential is expressed in terms of the time, one can calculate the corresponding electronic excitation by an approach similar to that used in the calculation of the stopping power, and thus a quantification of the results is to a certain extent possible. The probability of the electron excitation P_{KE} above the vacuum level is then given by

$$P_{\mathrm{KE}}=2\rho^2V^2\int_{\varepsilon_V}^{\infty}d\varepsilon_k T(\varepsilon_k)\int_{-\infty}^{\varepsilon_F}d\varepsilon_{k'}\times\left|\int_{-\infty}^{\infty}F(z(t))e^{i(\varepsilon_k-\varepsilon_{k'})t}dt\right|^2, \tag{3}$$

where ε_k and $\varepsilon_{k'}$ are energies of the electronic levels in the solid, the index k denotes a level above the vacuum level ε_V, and the index k' is a level below the Fermi level ε_F, respectively. The density of states ρ is assumed as constant. The factor 2 is due to the spin degeneracy and $T(\varepsilon_k)$ is the probability of transmission of an electron into the vacuum over the barrier of the height equal to $\varepsilon_V-\varepsilon_F$. Then we can assume $T(\varepsilon_k)$ in the form

$$T(\varepsilon_k)=\frac{1}{2}\left[1-\left(\frac{\varepsilon_V-\varepsilon_F}{\varepsilon_k-\varepsilon_F}\right)^{1/2}\right].$$

The potential $V(t)$ is expressed as a product $VF(t)$, where V is the perturbing potential inside the solid, and $F(z(t))$ is a suitable smooth function which is equal to unity inside the solid and decreases exponentially to zero outside the solid (z is the distance from the surface). A limiting choice for such a function is

$$F(t)=\frac{1}{\cosh(2\gamma v t)}, \tag{4}$$

which describes the basic character of the on/off switching of the interaction. It provides, after substitution of Eq. (4) into Eq. (3), the solution in the form

$$P_{\mathrm{sKE}}=4\rho^2V^2\left\{\ln(e^{\frac{-\pi W}{2\gamma v}}+1)-\pi^{1/2}\left(\frac{\pi W}{2\gamma v}\right)^{1/2}I\left[\left(\frac{\pi W}{2\gamma v}\right)^{1/2}\right]\right\} \tag{5}$$

where

$$I(x)=2\pi^{-1/2}\int_x^{\infty}\frac{dy}{e^{y^2}+1},$$

$W=\varepsilon_V-\varepsilon_F$, and the parameter γ describes the decay of V as the particle moves away from the solid (γ should be close to unity in atomic units), and is adjustable in our calculation. The absolute value of the product ρ^2V^2, which appears in Eqs. (3) and (5), is estimated quantitatively from Eq. (2) using the Lindhard-Scharff (LS) formula[19] corrected by the experimental data or from a more accurate theory for the electronic stopping power. Without these corrections the value of ρ^2V^2 cannot be evaluated with better accuracy than by a factor of 2. We should also mention that in Ref. 12 a simplified transmission function $T(\varepsilon_k)=1/2$ was used and the formula for P_{sKE} contained only the first summand on the right hand side of Eq. (5).

We have analyzed how formula (5) changes in dependence on the shape of function (4). We took a linear combination of indented functions (4), and obtained a pulse function with hyperbolic cosine like leading and trailing edges and a flat top. We evaluated Eq. (3) for this function on the computer, and found that the results are numerically almost the same as if directly calculated by using Eq. (5), which was derived for a peaklike function. Moreover, these results did not depend on the width of the pulselike function. This leads us to the conclusion that if a steplike function is used instead of pulselike or peaklike functions, the expression on the right-hand side of Eq. (5) should be divided by 2. The steplike function F is more adequate when the impinging particle penetrates into the solid, and there remains implanted. Therefore, the final formula for the sKE yield is given by

$$P_{\mathrm{sKE}}=2\xi\rho^2V^2\left\{\ln(e^{\frac{-\pi W}{2\gamma v}}+1)-\pi^{1/2}\left(\frac{\pi W}{2\gamma v}\right)^{1/2}\times I\left[\left(\frac{\pi W}{2\gamma v}\right)^{1/2}\right]\right\}, \tag{6}$$

where ξ is a correction factor for the values of ρ^2V^2 which are estimated using the LS theory. In Ref. 12 the factor ξ was inside the ρ^2V^2 value, and the theory was presented for only one adjustable parameter γ. For the Ne-Au system this seemed to be sufficient for fitting the sKE model to the experiment. However, for other systems the corrections to the LS values of ρ^2V^2 may not be known accurately enough, and therefore it is convenient to introduce ξ as a separate adjustable parameter, which has the meaning of a correction factor to the LS values of ρ^2V^2. Then the presented sKE model has two slightly varying (partially predictable) fitting parameters—γ and ξ.

Another important issue is the dependence of the yield P_{sKE} on the angle of electron emission and on the angle of projectile incidence. Because the angular dependencies of the $V_{kk'}$ matrix are not known, and to our knowledge no relevant experimental data are available, this problem remains unresolved at present.

We should stress that in the sKE model it is assumed for convenience that only the surface of the solid causes the semilocalization of the valence electrons. However, as we

mentioned above, the departure from the free-electron-like character of the valence electrons [cf. points (a) and (c) in Sec. I] leads to a similar localization and subsequently to a KE essentially indistinguishable from the one described by Eq. (6) except for a possibly different angular dependence. In summary, we list the main assumptions and features of the sKE model.

(i) It is a one-electron nonadiabatic model, where the excitation in the solid described by the matrix element $V_{kk'}$ plays the dominant role.

(ii) Due to the presence of the surface, the wave functions for the occupied $|k'\rangle$ level and unoccupied $|k\rangle$ level have a semilocalized character which determines the shape of the interaction matrix element $V_{kk'}$.

(iii) The perturbing potential has the character of an s scatterer, i.e., it does not depend on k and k', and hence $V_{kk'}=V$.

(iv) The time-dependent part of V can be modeled by a hyperbolic cosine function with one adjustable parameter γ.

(v) The squared product of V and ρ (density of states) is proportional to dE/dx (electronic stopping power in the target bulk). It is estimated from the Lindhard-Scharff theory and corrected by the second adjustable parameter ξ.

(vi) This model does not predict any threshold impact velocity for KE.

(vii) The angular dependence of the model remains to be clarified.

(viii) The transfer of excited electrons into the vacuum is represented by $T(\varepsilon_k)$ defined above.

(ix) The secondary electron excitation is neglected.

IV. APPLICATION OF THE sKE MODEL TO EXPERIMENTAL DATA ON Ne^+-Au, Ne^0-Au, O^+-Au, N^+-Au, C^+-Au, Xe^+-Au, and Au^+-Au

Results of our calculations of the total KE yield from Au bombarded by $Ne^{0,+}$, O^+, N^+, C^+, Xe^+, and Au^+ are shown in Figs. 2(a)–2(f) together with the respective experimental data.[7,11] In all experiments the incidence of the projectiles was perpendicular to the surface. The solid circles represent KE yields for the singly charged projectiles. For Ne^+ impact, these data were derived from the measured total PIE yields in Ref. 7 by subtracting a PE contribution, as explained in Ref. 20, whereas for impact of neutral projectiles Ne^0 the KE yield is as directly measured.[11] The carbon atom has a sufficiently low first ionization potential to neglect any PE for C^+ impact. For O^+-Au and N^+-Au collision systems, the PE yields are expected to be very small, and thus no large error is made if total KE yields are considered.

The solid heavy lines give the respective theoretical results from our sKE model. The input parameters for Eq. (6) are $W=5$ eV for all six collision systems, and $\rho^2V^2=29.8$, 22.8, 5.4, 4.4, 3.8, and 3.3 (the LS values) for the Au-Au, Xe-Au, Ne-Au, O-Au, N-Au, and C-Au, respectively.

For lighter systems best fits to the experimental data were obtained for $\gamma=1.45$, 1.6, 1.55, and 1.35 and $\xi=1.9$, 2.2, 2.1, and 2.3 for the systems Ne-Au, O-Au, N-Au, and C-Au, respectively. These fits are satisfactory up to $\sim$15 keV for all four collision systems, which shows that our model may also be relevant above the threshold velocity $v_{\mathrm{th},e}$. The vertical dashed lines in Fig. 2 indicate this threshold velocity. The good quantitative agreement for the four light projectile species between theory and experiment for projectile velocities below v_{th} indicates that the surface-assisted KE mechanism suggested in Ref. 12 can also explain subthreshold KE for the collision systems other than Ne-Au. The values for the adjustable parameters in the theory, which range from $\gamma=1.35$ to 1.6 a.u. and from $\xi=1.9$ to 2.3, are in reasonable agreement with theoretical expectations. However, the good agreement of the fits according to the sKE model with the experimental data still far above both $v_{\mathrm{th},e}$ and $v_{\mathrm{th},p}$ does not mean that the pKE mechanism does not contribute to KE in this region. One has to realize that all three KE mechanisms are nonadiabatic one-electron processes that cannot be experimentally separated, but could only be distinguished by their different thresholds, whereas far above the threshold all three of them will be present. The good fit with the sKE theory in the range from $E_{\mathrm{th},p}$ up to $\sim$15 keV can mean either an underestimated value of $v_{\mathrm{th},p}$ or that the fitting parameters in Eq. (6) may be incorrect and thus compensate for the missing pKE contribution. To be more specific, when characterizing the pKE model as a one-electron process we regarded only one excitation path for this mechanism, namely, direct promotion of the diabatic level into the continuum with one-step autoionization. Another excitation path involves creation of a core-level vacancy followed by Auger de-excitation, which is a two-step mechanism with a two-electron process as the second step.

For the heavier collision systems Xe^+-Au and Au^+-Au a clear discrepancy between predictions of the one-electron theories and the experimental data is observed. Taking into consideration the constraints for the parameters ξ and γ, no good fit of the sKE model predictions to the low impact energy range shown in Figs. 2(e) and 2(f) can be made. For these fits (solid heavy line), Eq. (6) was used. The fitting parameters are $\gamma=2.0$ and 1.5 and $\xi=0.55$ and 0.28 for the Xe-Au and Au-Au systems, respectively. We conclude that neither the sKE model nor any other one-electron model mentioned so far can explain the occurrence of subthreshold KE in the very low impact velocity region where the KE yield γ_{KE} depends only very weakly on the impact velocity and actually almost levels off. In Sec. V our model for interpreting these very low impact velocity KE data [shown in Figs. 2(e) and 2(f)] will be introduced.

V. MANY-ELECTRON SURFACE-ASSISTED KE

We assume that electronic excitation is caused by binary collisions of the moving projectile with free-electron-gas electrons in the target. We further assume that these collisions occur only close to or right at the surface, i.e., a (semi)localization of the electron wave functions of the solid due to the presence of the surface, as for the sKE model.[12] The energy deposited by a moving particle in the free-electron gas near the surface is then given by

$$E=\rho^2V^2\int_{\varepsilon_F}^{\infty}d\varepsilon_k\int_{-\infty}^{\varepsilon_F}d\varepsilon_{k'}(\varepsilon_k-\varepsilon_{k'})\times\left|\int_{-\infty}^{\infty}F(z(t))e^{i(\varepsilon_k-\varepsilon_{k'})t}dt\right|^2. \tag{7}$$

After substitution of Eq. (4) into Eq. (7) we obtain the analytical solution $E=\frac{4}{3}\pi\rho^2V^2\gamma v$. If for F we take a step-

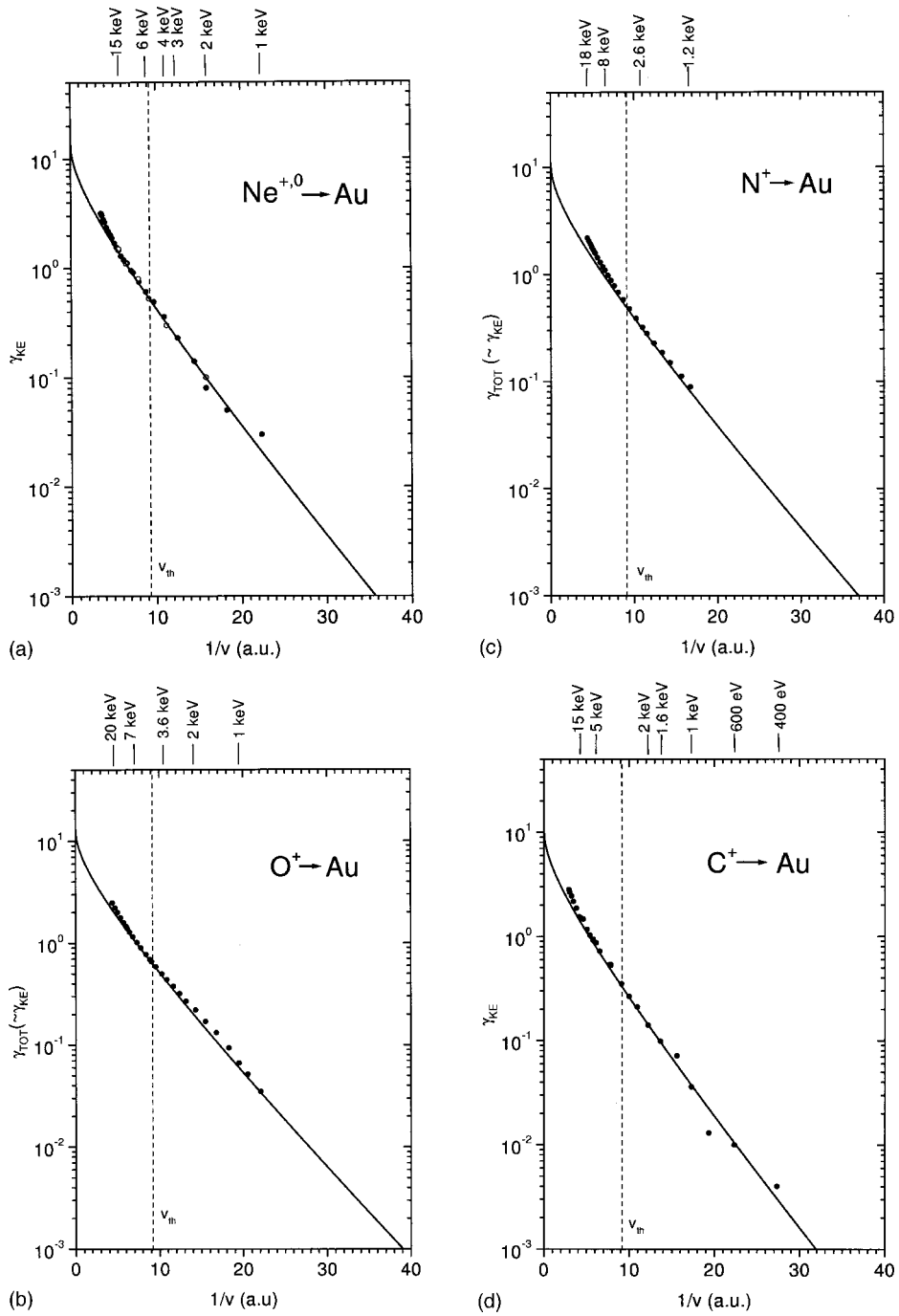

FIG. 2. KE yields γ_{KE} for the collision systems (a) $Ne^{0,+}$-Au (Ref. 12), (b) O^+-Au, (c) N^+-Au, (d) C^+-Au, (e) Xe^+-Au, and (f) Au^+-Au in dependence on the inverse impact velocity. Solid circles represent the experimental data for singly charged projectiles (Refs. 6–8), and open circles in (a) for the Ne^0 projectiles (Ref. 11). The solid lines are the result of calculations based on Eq. (6), with the parameters described in the text. The vertical dashed line defines the beginning of the subthreshold velocity region ($v_{th} \approx 2.4 \times 10^5$ m/s or 0.11 a.u.). Impact energies corresponding to selected impact velocities on the x axis are indicated by arrows on top of the figures. The dotted lines in Figs. 2(e) and 2(f) represent our fits using Eq. (13), with parameters as explained in the text.

like function instead of a peaklike one, with a similar shape for switching on as in Eq. (4), the solution for E should be divided by 2. The total energy deposited at the surface in the form of electron-hole excitation of the Fermi gas is then given by

$$E = \frac{2}{3}\pi\rho^2 V^2 \gamma v. \tag{8}$$

This energy is redistributed among the excited electrons by the distribution function

$$P(\varepsilon_k) = \frac{\pi\rho^2 V^2}{\gamma v} \frac{1}{e^{(\pi/2\gamma v)(\varepsilon_k - \varepsilon_F)} + 1}. \tag{9}$$

This function reminds us of the Fermi-Dirac distribution, where instead of the temperature a parameter $2\gamma v/\pi$ is used

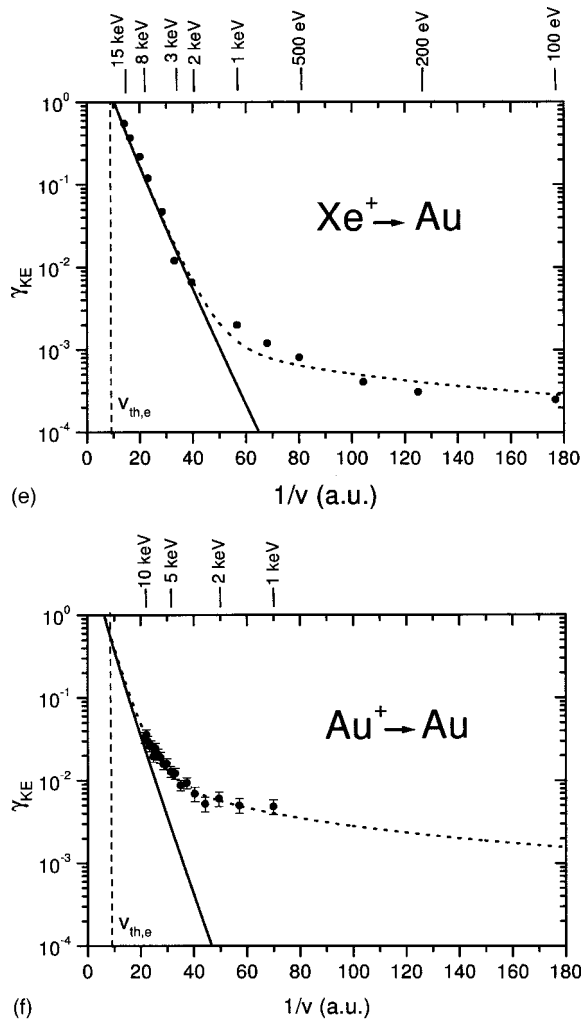

FIG. 2. (*Continued*).

which characterizes the broadening of the electron energy distribution due to the Heisenberg uncertainty principle. If Eq. (9) is multiplied by $T(\varepsilon_k)$ and integrated over ε_k from ε_V to ∞, one obtains Eq. (6) with $\xi=1$. We have already shown in Sec. IV that the experimental data in Figs. 2(e) and 2(f) at very low impact energy cannot be well fitted by Eq. (6), which corresponds to energy distribution (9) multiplied by $T(\varepsilon_k)$, because this energy distribution is too narrow to explain the KE induced by slow heavy particles. In order to interpret these experimental data, we must suppose that the distribution of the excited electrons (or at least a part of it) is broadened. A possible source of this $P(\varepsilon_k)$ broadening is electron-electron (*e-e*) interaction. The key assumption for such *e-e* interaction to be relevant is the localization of the electronic excitation in the impact zone. If the particle is slow enough, its passage through the surface takes a comparably long time, and the perturbation of the Fermi gas near the surface of the solid will last accordingly longer (some fs), which may be sufficient for electrons to be energetically redistributed through *e-e* interaction. This *e-e* interaction, however, does not change the amount of energy [Eq. (8)] deposited by the projectile at the surface. Further we assume that the redistributed energy distribution consists of two parts.

The first part is equivalent to Eq. (9), and the second part is assumed to have the form $\sim a(v)\exp[-(\varepsilon_k-\varepsilon_F)/\varepsilon_0]$, where a is a function of v and ε_0 is a new parameter. For very small impact velocities the latter part dominates, and must yield the total deposited energy [Eq. (8)] at the lowest impact velocities. Then the function a can be found from the equation

$$\int_{\varepsilon_F}^{\infty} a(v)e^{-(\varepsilon_k-\varepsilon_F)/\varepsilon_0}(\varepsilon_k-\varepsilon_F)d\varepsilon_k=\frac{\pi}{3}\rho^2V^2\gamma v, \quad (10)$$

where only one-half of E from Eq. (8) is on the right-hand side of Eq. (10), because the integral in Eq. (10) includes only the excitation for electrons, whereas Eq. (8) covers both electrons and holes. The function a is then given by

$$a(v)=\frac{\pi\rho^2V^2\gamma v}{3\varepsilon_0^2}. \quad (11)$$

Finally, the redistributed energy distribution for electron-hole excitation is

$$P(\varepsilon_k)=\rho^2V^2\left[\frac{\pi}{\gamma v}\frac{1}{e^{(\pi/2\gamma v)(\varepsilon_k-\varepsilon_F)}+1}+\frac{\pi\gamma v}{3\varepsilon_0^2}e^{-(\varepsilon_k-\varepsilon_F)/\varepsilon_0}\right], \quad (12)$$

where ε_0 can be interpreted as a parameter characterizing the width of the energy distribution of the redistributed part of the excited electrons. The parameter ε_0 probably increases slightly with increasing v as in the model described in Ref. 21. However, because the mechanism of the energy redistribution is not precisely known, for simplicity we assume ε_0 = const. For small velocities the parameter ε_0 is larger than the energy uncertainty $2\gamma v/\pi$, and the second term on the right-hand side of Eq. (12) will dominate. For larger velocities, on the other hand, the first term on the right-hand side of Eq. (12) will be dominant. As Eq. (12) is not properly normalized, it gives slightly higher values at intermediate energies. Multiplying Eq. (12) by $T(\varepsilon_k)$ and integrating over ε_k from ε_V to ∞ gives an equation for the electron emission yield:

$$P_{\mathrm{mKE}}=2\xi\rho^2V^2\left\{\ln(e^{\frac{-\pi W}{2\gamma v}}+1)-\pi^{1/2}\left(\frac{\pi W}{2\gamma v}\right)^{1/2}I\left[\left(\frac{\pi W}{2\gamma v}\right)^{1/2}\right]\right.$$
$$\left.+\frac{\pi\gamma v}{6\varepsilon_0}\left[e^{-\frac{W}{\varepsilon_0}}-\pi^{1/2}\left(\frac{W}{\varepsilon_0}\right)^{1/2}erfc\left(\left(\frac{W}{\varepsilon_0}\right)^{1/2}\right)\right]\right\}, \quad (13)$$

where *erfc(x)* is the complementary error function. The integration itself yields a formula without ξ (i.e., with $\xi=1$). The ξ parameter has to be introduced for fitting as in case of Eq. (6) because the ρ^2V^2 value cannot be predicted with better accuracy than by a factor of ~ 2. Equation (13) can be directly compared with the measured electron yields.

The many-electron model proposed here can also be viewed as an extension of the one-electron sKE model, since for $\varepsilon_0=0$ Eq. (13) reduces to Eq. (6). This mechanism includes a many-electron process for redistribution of the excitation energy. We label this model mKE.

As for the sKE mechanism, the angular dependence of the mKE model remains open. Let us summarize the main assumptions and features of this model.

(i) It is a parametric many-electron model.

(ii) First the electrons are excited by a one-electron excitation process described by the sKE mechanism, i.e., the

model involves the same shape (a hyperbolic cosine function with parameter γ) and character (s scatterer) of the matrix element $V_{kk'}$, and the same semilocalization of the electron wave functions $|k\rangle$ and $|k'\rangle$ due to their spatial constraint imposed by the surface.

(iii) Due to the slow passage of the projectile through the surface, this excitation can remain localized for a sufficiently long time ($\sim 10^{-15}$–10^{-14} s) in the impact zone at the target surface, during which time fast electron-electron interactions (with a time constant of $\sim 10^{-16}$ s) can cause an energetic broadening of the excited electron distribution.

(iv) This energetic broadening can be characterized by a function according to Eq. (12), with the adjustable parameter ε_0.

VI. APPLICATION OF THE mKE MODEL TO MEASURED ELECTRON YIELDS FOR IMPACT OF Xe^+ AND Au^+ ON Au

These two projectile ions have such a low potential energy that no PE from Au is possible,[6,8,16] and therefore genuine KE yields are measured. The dotted lines represent best fits of Eq. (13) to these experimental data. The input and fitting parameters for Eq. (13) are: $W=5$ eV for both systems, $\gamma=$ 2.0 and 1.5, $\xi=0.55$ and 0.28, $\rho^2V^2=22.8$ and 29.8, and $\varepsilon_0=0.026$ and 0.04 for Xe^+-Au and Au^+-Au, respectively. The solid lines are for $\varepsilon_0=0$. As demonstrated in Figs. 2(e) and 2(f), these fits are very satisfactory at both boundaries of the considered impact energy region. In the intermediate range the fit is not that good, because the distribution function (12) was normalized to the total deposited energy only in the high- and low-velocity regions but not for intermediate velocities. The theoretical description in the intermediate region can be improved by inclusion of a proper explicit dependence of ε_0 on v, e.g., $\varepsilon_0 \propto \sqrt{v}$ as in Ref. 21.

Our theory provides a physical interpretation underlying Eq. (13) which imposes constraints on the values of the fitting parameters. The parameter γ between 1 and 2 and $\varepsilon_0 \approx 0.71$ and 1.1 eV are physically reasonable values.

VII. CONCLUSIONS

We have shown that a mechanism of surface-assisted KE (sKE) can explain experimental observations in the subthreshold velocity region for KE from clean polycrystalline Au bombarded by $Ne^{0,+}$, O^+, N^+, and C^+. Because the excited electrons originate from the valence band of the solid, this mechanism is related to the electronic stopping power. However, the main difference is that the sKE mechanism has no cutoff projectile velocity as a consequence of the semilocalization of valence-band wave functions by the surface. The sKE mechanism belongs to one-electron models which go beyond the idealized free-electron-gas theories.

For the explanation of very low impact velocity data, where a conspicuous leveling off of the KE yield occurs, a phenomenologically introduced many-electron surface-assisted KE mechanism (mKE) was used. The mKE can explain the measured KE yields (deep in the subthreshold region) from clean polycrystalline Au bombarded by very slow Xe^+ and Au^+ ions. The fits of this model to the experimental data result in physically reasonable values for the microscopic parameters. We assume for convenience that the key role in both the sKE and mKE models is played by the surface, because the latter provides a spatial localization of the electron wave functions and a temporal localization of the electronic excitation, which are the main features of the model. This localization leads to a broadening of the energy distribution by electron-electron interaction, and thus facilitates the emission of electrons at very low impact energies.

ACKNOWLEDGMENTS

This work was supported by a KONTAKT grant for bilateral cooperation between the Czech Republic and Austria, and also partly by Grant Nos. 7801 of AV ČR and 202/99/0881 of GAČR. Work on the Austrian side was carried out within Association EURATOM-OEAW, and was supported by Fonds zur Förderung der wissenschaftlichen Forschung (FWF).

[1] M. Rösler, W. Brauer, J. Devooght, J.-C. Dehaes, A. Dubus, M. Cailler, and J.-P. Ganachaud, *Particle Induced Electron Emission I* (Springer, Berlin, 1991), and references therein.

[2] D. Hasselkamp, H. Rothard, K.-O. Groeneveld, J. Kemmler, P. Varga, and HP. Winter, *Particle Induced Electron Emission II* (Springer, Berlin, 1992), and references therein.

[3] R. Baragiola, in *Low Energy Ion-Surface Interactions*, edited by J. W. Rabalais (Wiley, New York, 1994), Chap. 4, p. 188, and references therein.

[4] B. A. Trubnikov and Yu. N. Yavlinski, Zh. Eksp. Teor. Fiz. **48**, 253 (1965) [Sov. Phys. JETP **21**, 167 (1965)].

[5] R. A. Baragiola, E. V. Alonso, and A. Oliva Florio, Phys. Rev. B **19**, 121 (1979).

[6] H. Eder, W. Messerschmidt, HP. Winter, and F. Aumayr, J. Appl. Phys. **87**, 8198 (2000).

[7] H. Eder, F. Aumayr, and HP. Winter, Nucl. Instrum. Methods Phys. Res. B **154**, 185 (1999).

[8] G. Lakits, F. Aumayr, M. Heim, and HP. Winter, Phys. Rev. A **42**, R5780 (1990).

[9] U. Wille and R. Hippler, Phys. Rep. **132**, 129 (1986).

[10] L. Guillemot, S. Lacombe, V. N. Tuan, V. A. Esaulov, E. Sanchez, Y. A. Bandurin, A. I. Dashchenko, and V. G. Drobnich, Surf. Sci. **365**, 353 (1996).

[11] G. Lakits, A. Arnau, and HP. Winter, Phys. Rev. B **42**, 15 (1990).

[12] J. Lörinčík and Z. Šroubek, Nucl. Instrum. Methods Phys. Res. B **164–165**, 633 (2000).

[13] G. Spierings, I. Urazgil'din, P. A. Zeijlmans van Emmichoven, and A. Niehaus, Phys. Rev. Lett. **74**, 4543 (1995).

[14] M. J. Frisch, G. W. Trucks, H. B. Schlegel, G. E. Scuseria, M. A. Robb, J. R. Cheeseman, V. G. Zakrzewski, J. A. Montgomery, Jr., R. E. Stratmann, J. C. Burant, S. Dapprich, J. M. Millam, A. D. Daniels, K. N. Kudin, M. C. Strain, O. Farkas, J. Tomasi, V. Barone, M. Cossi, R. Cammi, B. Mennucci, C. Pomelli, C. Adamo, S. Clifford, J. Ochterski, G. A. Petersson, P. Y. Ayala,

Q. Cui, K. Morokuma, D. S. Malick, A. D. Rabuck, K. Raghavachari, J. B. Foresman, J. Cioslowski, J. V. Ortiz, B. B. Stefanov, G. Liu, A. Liashenko, P. Piskorz, I. Komaromi, R. Gomperts, R. L. Martin, D. J. Fox, T. Keith, M. A. Al-Llaham, C. Y. Peng, A. Nanayakkara, C. Gonzalez, M. Challacombe, P. M. W. Gill, B. Johnson, W. Chen, M. W. Wong, J. L. Andres, C. Gonzalez, M. Head-Gordon, E. S. Replogle, and J. A. Pople, Gaussian 98, Rev. A.6, Gaussian, Inc., Pittsburgh, PA, 1998.

[15] P. J. Hay and W. R. Wadt, J. Chem. Phys. **80**, 270 (1985).

[16] E. V. Alonso, M. A. Alurralde, and R. A. Baragiola, Surf. Sci. **166**, L155 (1986).

[17] J. A. Yarmoff, T. D. Liu, S. R. Qiu, and Z. Sroubek, Phys. Rev. Lett. **80**, 2469 (1998).

[18] G. Falcone and Z. Šroubek, Phys. Rev. B **39**, 1999 (1989).

[19] J. Lindhard and M. Scharff, Phys. Rev. **124**, 128 (1961).

[20] H. Eder, M. Vana, F. Aumayr, and HP. Winter, Rev. Sci. Instrum. **68**, 165 (1997).

[21] Z. Šroubek, Phys. Rev. Lett. **78**, 3204 (1997).